

# Ultrafast dynamics and interlayer thermal coupling of hot carriers in epitaxial graphene

Dong Sun<sup>\*1</sup>, Zong-Kwei Wu<sup>1</sup>, Charles Divin<sup>1</sup>, Xuebin Li<sup>2</sup>, Claire Berger<sup>2</sup>, Walt A. de Heer<sup>2</sup>, Phillip N. First<sup>2</sup>, and Theodore B. Norris<sup>1</sup>

<sup>1</sup> Center for Ultrafast Optical Science, University of Michigan, 2200 Bonisteel Blvd., 48109, Ann Arbor, USA

<sup>2</sup> School of Physics, Georgia Institute of Technology, 30332, Atlanta, USA

Received 30 June 2008, accepted 21 August 2008

Published online 28 October 2008

PACS 42.62.Fi, 73.21.Ac, 78.47.J-

\* Corresponding author: e-mail sundong@umich.edu, Phone: +001 734 709 3982, Fax: +001 734 763 4876

We report the first application of nondegenerate ultrafast pump-probe spectroscopy to investigate the dynamics of hot Dirac Fermions in epitaxial graphene. The DT spectra can be understood in terms of the effect of hot thermal carrier distributions on interband transitions with no electron-hole interaction.

We also investigate the thermal coupling between carriers of doped and undoped layers. The coupling time is found to be below 500fs.

© 2009 WILEY-VCH Verlag GmbH & Co. KGaA, Weinheim

**1 Introduction** Two-dimensional graphene layers are the subject of considerable research at present, due to their unusual band structure and the potential for future electronic-device applications [1-3]. In particular, graphene grown epitaxially on SiC substrates and patterned via standard lithographic procedures has been proposed as a platform for carbon-based nanoelectronics and molecular electronics [1-3]. In high-speed devices, hot electrons are generated due to the presence of time-dependent high electric fields. It is critical therefore to understand both the cooling of the electrons due to coupling to lattice phonons, and the coupling of different layers in epitaxial graphene samples. Here we report the first nondegenerate ultrafast spectroscopic measurements of the dynamics of Dirac quasiparticles in graphene in the region near the Fermi level.

**2 Experiment** The sample is an ultrathin epitaxial graphene film produced on the C-terminated face of single-crystal 4H-SiC by thermal desorption of Si. Details of the growth process and sample characterization have been discussed elsewhere [1]. The structure of the sample is shown in Fig. 1; it consists of multiple layers containing one doped and multiple undoped graphene sheets. A 100-fs near-infrared (800-nm) optical pulse (from a 250-kHz regenerative amplifier) excites quasiparticles from the va-

lence to the conduction band across the Dirac point; the optical response is measured via the differential transmission (DT) of a mid-infrared probe pulse from a tunable femtosecond OPA as a function of pump-probe delay. The elevated temperature of the quasiparticles is manifested primarily through the modification of the probe beam absorption by Pauli blocking of interband transitions.

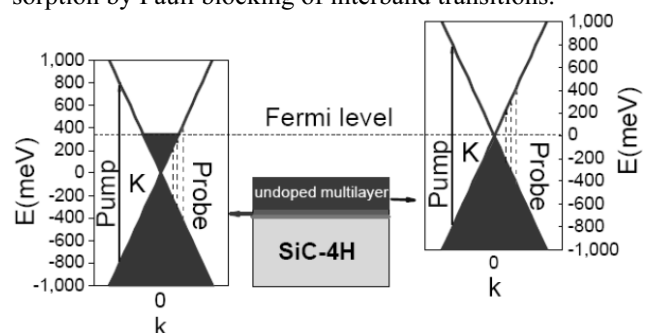


**Figure 1** Sample structure and energy dispersion. The sample has a buffer layer on the SiC substrate followed by 1 heavily doped graphene layer and approximately 20 undoped layers. The Fermi level is indicated by the horizontal dashed line. The solid vertical line shows the transitions induced by the 800-nm optical pump pulse; the three dashed lines correspond to probe transitions at different energies with respect to the Fermi level.

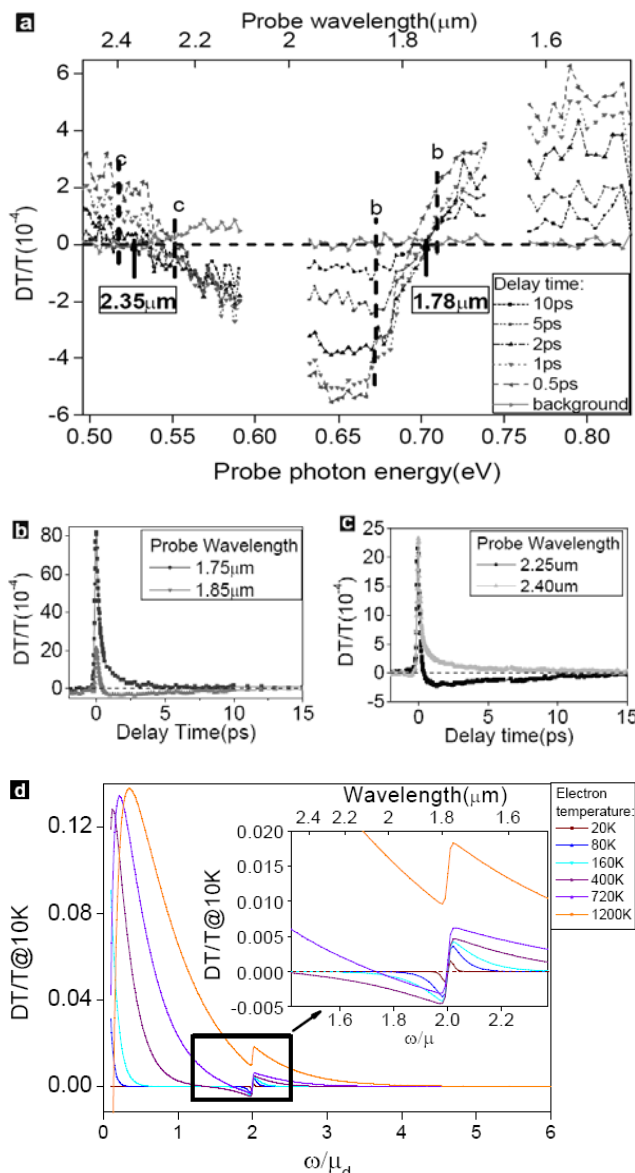


**Figure 2** a) DT spectrum on epitaxial graphene at 10 K, with 500- $\mu$ W 800-nm pump with sub-100-fs pulse width at probe delays of 10 ps, 5 ps, 2 ps, 1 ps, 0.5 ps and background (50 ps before the pump arrives). b) DT time scan at the two probe wavelengths marked in part a at the red (1.85  $\mu$ m) and blue side (1.75  $\mu$ m) of the 1.78  $\mu$ m DT zero crossing. c) Time scan of the two probe wavelengths marked in part a at the red (2.40  $\mu$ m) and blue side (2.25  $\mu$ m) of the 2.35  $\mu$ m DT zero crossing. In all figures, the dashed line marks where the DT signal is zero. d) Simulated DT/T curves at different electron temperatures with a lattice temperature of 10 K. In the inset, the DT/T curves for low electron temperatures are expanded in the vicinity of the two DT zero crossings.

### 3 Results and discussion

**3.1 DT spectra** Figure 2a shows DT spectra for a single position on the epitaxial graphene sample at various probe time delays, for a substrate temperature of 10 K and 500- $\mu$ W pump power. The most notable feature of the DT

spectrum is the two zero crossings, at 1.78  $\mu$ m and 2.35  $\mu$ m respectively. Figures 2(b) and (c) show DT time scans for selected probe wavelengths on both sides of the two zero crossings. Immediately following the pump pulse at time zero, the DT signal is positive over the entire probe spectral range. The DT signal becomes negative within 2 ps if the probe wavelength falls between the two zero crossings; otherwise it remains positive until the signal decays away. The DT signal relaxes to zero on a time scale of 1-10 ps depending on probe wavelength. The lack of the data in the two blank regions of Fig. 1(a) is due to limitations in tuning our OPA.

The differential probe transmission spectrum arises mainly from the change in carrier occupation functions in the bands. Following the excitation of quasiparticles high into the conduction band by the pump pulse, electron-electron scattering on a time scale short compared to 150 fs establishes a hot thermal distribution characterized by an electron temperature  $T_e$ . Since the carrier occupation probability above the Fermi energy is increased, the DT signal is positive due to reduced probe absorption. The probe DT is negative below the Fermi level, however, since the heating of the electron plasma reduces the occupation probability for low energies. Thus the upper zero crossing at 1.78  $\mu$ m probe wavelength is interpreted as arising from the smearing of the Fermi level in the doped layers. Assuming no bandgap (or any possible bandgap to be less than the probe energy), we find the Fermi level to be 348 meV above the Dirac point for the doped layer. We note additionally that there is no peak in the DT spectrum near the Fermi level; this indicates that there is no Fermi edge singularity [4, 5] due to electron-hole interactions in the inter-band absorption spectrum of graphene, as may be expected from the massless nature of the quasiparticles. At very long probe wavelengths, i.e. for transition final states well below the Fermi level of the doped layers, one may expect the DT spectra to be determined primarily by the carrier occupations in the undoped layers; since the pump pulse generates hot carriers in the undoped layers, the sign of the DT signal arising from the undoped layers should be positive for all wavelengths. However, for probe wavelengths below the Fermi level of the doped layer, the contribution of the doped layer to the DT is negative. Thus one expects that for some probe energy the net DT signal should flip sign; this is the origin of the lower zero crossing at 2.35  $\mu$ m.

Figure 2(d) shows the simulated DT/T curves at different electron temperatures for a lattice temperature of 10 K, using a transfer matrix calculation [6] incorporating the theoretical electron-temperature-dependent dynamic conductivity [7]. The simulated DT spectra show upper and lower zero crossings at energies ( $2\mu_d$  and  $1.5\mu_d$  respectively,  $\mu_d$  is the energy of the Fermi level above the Dirac point in the doped layer) close to those observed in the experiment. (The experimental DT spectra are not calibrated, so there is an undetermined magnitude difference relative to the DT/T simulation. Additional simulations performed

by excluding various contributions to the total conductivity reveal that our DT spectra are well described by interband transitions and the single-particle density of states for linear dispersion, and no electron-hole interaction.

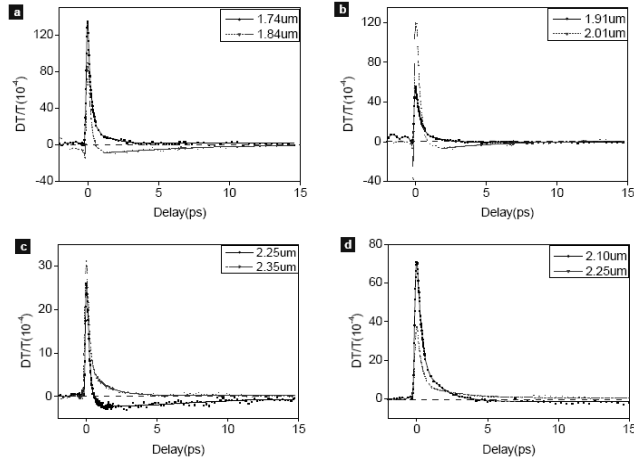


**Figure 3** DT time scans taken on different positions of the sample; a) and b) show the upper zero crossing shifts at two different positions of the sample. c) and d) Shifts of the other lower zero crossing points at two different positions of the sample. All the data are taken at 10 K, with 500- $\mu$ W 800-nm pump. The dashed line marks where the DT signal is zero. All the DT tails are simply fitted by sigmoidal curve as a guide to the eye.

DT spectra and time scans were taken at various positions on the sample over several square millimeters of area, revealing the effects of inhomogeneity [8]. The effect of the varying Fermi level on the DT time scans is shown in Fig. 3 above. Shifts of the DT zero crossings with position showed that the Fermi energy varies by as much as 35 meV across the sample surface.

**3.2 Fitting of the cooling dynamics** Using the transfer matrix results, which enable us to deduce the carrier temperature from the DT signal, it is possible for us to work backwards and obtain the carrier temperature as a function of time from the DT time scans. The simplest possible model for the thermal dynamics is to assume an exponential decay of the electron temperature following the fast initial thermalization in the first 120 fs. At probe wavelengths close to the upper zero crossing point, the data can be well fitted by an exponential decay function:  $T_e(t) - T_1 = (T_e^i - T_1) \cdot \exp(-t/\tau)$  with initial electron temperature of  $T_e^i = 1335$  K and time constant  $\tau = 1.45$  ps,  $T_1 = 10$  K is the lattice temperature. The fitting result is shown in Figs. 4a and 4b.

Attempts to fit the DT/T time scan for probe wavelengths around the lower zero crossing point assuming exponential temperature dynamics failed. The simplest model which fit the data well was to assume a stretched exponential decay function:  $T_e(t) - T_1 = (T_e^i - T_1) \cdot \exp(-t/\tau)^{1/h}$ . The fitting result is shown in Fig. 4c with  $h = 3$ ,  $T_e^i = 865$  K,  $\tau = 4$  ps. We cannot yet conclude whether the origin of the

stretched exponential behaviour is due to disorder, the temperature-dependence of the electron-phonon interaction, or the generation of hot phonons. At even lower energies, e.g. at 2.4  $\mu$ m, the DT/T time scans cannot be well-fit even by a stretched exponential decay function. Due to sample inhomogeneity the electron temperature relaxation time constant for the decay varies considerably for different positions on the sample; as an illustration Fig. 4(d) below shows another position which has  $T_e^i = 750$  K,  $\tau = 11$  ps. In all the fittings, the electron temperature relaxes to about 420 K at 1.7 ps by emitting two or three 197 meV optical G phonons [9], or one to two 330 meV D phonons [10, 11]. The relaxation afterwards is mainly due to the relatively slow acoustic phonon scattering process.

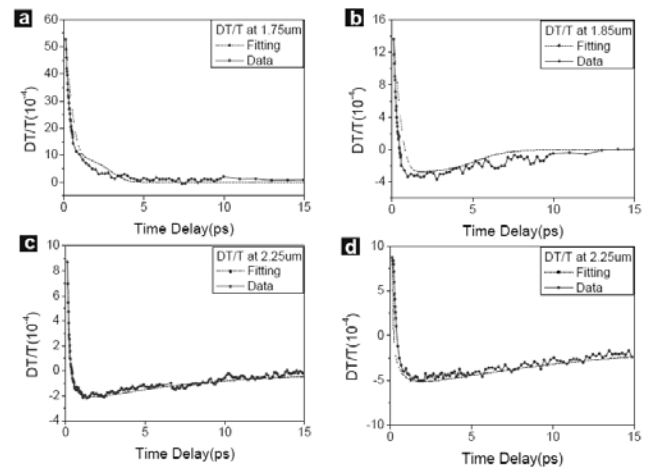


**Figure 4** DT/T signal fits. a), b) DT/T signal fits around upper zero crossing point at probe wavelengths of 1.75  $\mu$ m and 1.85  $\mu$ m; the electron temperature fitting function is  $T_e(t) - 10$  K =  $(1335$  K -  $10$  K)  $\cdot \exp(-t/1.45$  ps). c) DT/T signal fit around the lower zero crossing point at probe wavelength of 2.25  $\mu$ m, the electron temperature fitting function is  $T_e(t) - 10$  K =  $(865$  K -  $10$  K)  $\cdot \exp(-t/4\text{ps})^{1/3}$ . d) DT/T fit around the lower zero crossing at probe wavelength of 2.25  $\mu$ m at a different position on the sample from c; the electron temperature fitting function is  $T_e(t) - 10$  K =  $(750$  K -  $10$  K)  $\cdot \exp(-t/11\text{ps})^{1/3}$ .

**3.3 Number of undoped layers and DT spectra zero crossings**

In simulations incorporating varying numbers of undoped layers, we studied the behaviour of the dependence of two zero crossing positions on number of undoped layers. The upper zero crossing arises simply from the position of the Fermi level in the doped layer of the multilayer graphene sample, so it doesn't move when the number of undoped layers is changed in the simulation (Fig. 5). The lower zero crossing occurs where the positive DT arising from the thermally excited carriers in the undoped layers equals the negative DT arising from the smearing of the Fermi distribution in the doped layer induced by the pump pulse. The position of the lower zero crossing shifts to higher energy monotonically with the number of undoped layers. The shift is large for the first few undoped layers, but becomes fairly insensitive to the

number of layers above about fifteen layers. Our best estimate for the number of undoped layers is 20. The presence of the lower zero crossing is extremely strong evidence that thermally grown carbon-face epitaxial graphene on SiC contains several undoped layers as well as the doped layer lying nearest the substrate.

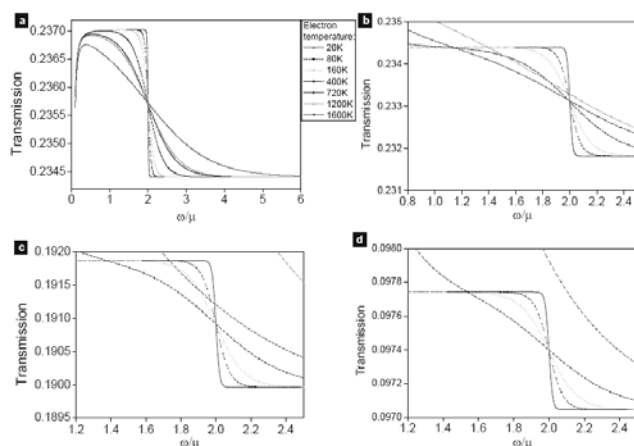


**Figure 5** Zero crossings shift with the number of undoped layers. a) Transmission spectrum with no undoped layers and b) transmission spectrum with 1 undoped layer. c) Transmission spectrum with 20 undoped layers. d) Transmission spectrum with 100 undoped layers. All the figures share the same legend.

### 3.4 Thermal coupling between carriers in the doped and undoped layers

To study the thermal coupling of carriers between the doped and undoped layers, we used 1.9- $\mu\text{m}$  pump pulses from the idler of the OPA to selectively excite hot carriers in the undoped layers of another sample with 62 undoped layers. The Fermi level in the doped layer is found to be 360 meV above the Dirac point by the position of the first zero crossing, so the pump photon will not excite the carriers in the doped layer directly due to Pauli blocking. The observation of DT signals with probe wavelength at 1.32  $\mu\text{m}$  (Fig. 6) indicates smearing of the Fermi level in the doped layer, whose energy comes from the hot carriers excited in the undoped layers. The two-photon cross correlation signal taken on a GaAs sample (Fig. 6) under the same conditions is used as a reference. The rise time of the DT signal indicates the initial heat transfer between the undoped and doped layers is less than 500 fs. Possible thermal coupling mechanisms can be c-axis optical phonons, coupling between in-plane optical phonons, and the coupling between electronic states in different layers by disorder.

**4 Conclusion** We have observed the ultrafast relaxation dynamics of hot Dirac fermionic quasiparticles in multilayer epitaxial graphene. The DT spectra are well described by interband transitions with no electron-hole interaction. Following the initial thermalization and emission of high-energy phonons, the cooling is determined by electron-acoustic phonon scattering on the time scale of 1 ps for highly doped layers, and 4–11 ps in undoped layers.

The scattering with acoustic phonons is relevant to graphene-based electronic devices operating at not-too-high fields. The coupling of the hot carriers from the undoped layers to doped layer in epitaxial graphene was observed. The coupling time is below 500 fs.

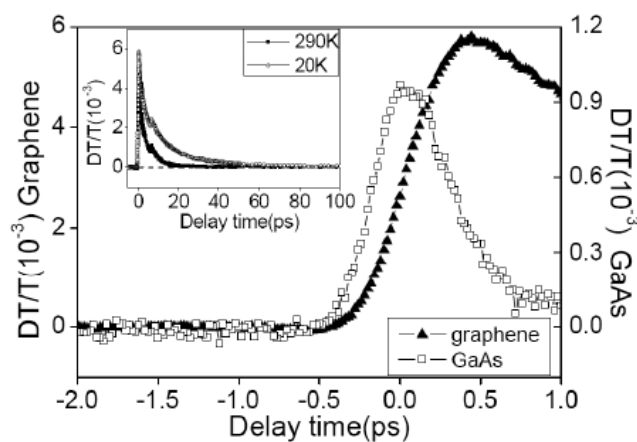


**Figure 6** DT signal of 1.9  $\mu\text{m}$  pump (0.3 mW) and 1.32  $\mu\text{m}$  probe on graphene (62 undoped layers) and GaAs at 20 K around time zero. The inset is the DT signal on graphene at lattice temperatures of 10 K and 290 K.

**Acknowledgements** This project has been supported by NSF grants ECCS-0404084 and ECCS-0521041.

### References

- [1] M. L. Sadowski, G. Martinez, M. Potemski, C. Berger, and Walt A. de Heer, *Solid State Commun.* **143**, 123 (2007).
- [2] C. Berger, Zhimin Song, Xuebin Li, Xiaosong Wu, Nate Brown, Cecile Naud, Didier Mayou, Tianbo Li, Joanna Hass, A. N. Marchenkov, E. H. Conrad, P. N. First, and W. A. de Heer, *Science* **312**, 1191 (2006).
- [3] K. S. Novoselov, A. K. Geim, S. V. Morozov, D. Jiang, Y. Zhang, S. V. Dubonos, I. V. Grigorieva, and A. A. Firsov, *Science* **306**, 666 (2007).
- [4] H. Kalt, K. Leo, R. Cingolani, and K. Ploog, *Phys. Rev. B* **40**, 12017 (1989).
- [5] T. Uenoyama and L. J. Sham, *Phys. Rev. Lett.* **65**, 1048 (1990).
- [6] M. Born and E. Wolf, *Principles of Optics: Electromagnetic Theory of Propagation, Interference and Diffraction of Light*, 7th ed. (Cambridge University Press, 1999).
- [7] S. A. Mikhailov and K. Ziegler, *Phys. Rev. Lett.* **99**, 016803 (2007).
- [8] J. Martin, N. Akerman, G. Ulbricht, T. Lohmann, J. H. Smet, K. von Klitzing, and A. Yacoby, *Nature Phys.* **4**, 144 (2008).
- [9] C. Faugeras, A. Nerière, M. Potemski, A. Mahmood, E. Dujardin, C. Berger, and W. A. de Heer, *Appl. Phys. Lett.* **92**, 011914, (2008).
- [10] S. Butscher, F. Milde, M. Hirtschulz, E. Malic, and A. Knorr, *Appl. Phys. Lett.* **91**, 203103 (2007).
- [11] T. Kampfrath, L. Perfetti, F. Schapper, C. Frischkorn, and M. Wolf, *Phys. Rev. Lett.* **95**, 187403 (2005).